## Ionospheric effects of the solar flares of September 23, 1998 and July 29, 1999 as deduced from global GPS network data

Afraimovich E. L., Altyntsev A. T., Kosogorov E. A., Larina N. S., and Leonovich L. A.

Institute of Solar-Terrestrial Physics SD RAS, p. o. box 4026, Irkutsk, 664033, Russia fax: +7 3952 462557; e-mail: afra@iszf.irk.ru

#### Abstract

This paper presents data from first GPS measurements of global response of the ionosphere to solar flares of September 23, 1998 and July 29, 1999. The analysis used novel technology of a global detection of ionospheric effects from solar flares (GLOBDET) as developed by one of the authors (Afraimovich E. L.). The essence of the method is that use is made of appropriate filtering and a coherent processing of variations in total electron content (TEC) in the ionosphere which is determined from GPS data, simultaneously for the entire set of visible (over a given time interval) GPS satellites at all stations used in the analysis. It was found that fluctuations of TEC, obtained by removing the linear trend of TEC with a time window of about 5 min, are coherent for all stations and beams to the GPS satellites on the dayside of the Earth. The time profile of TEC responses is similar to the time behavior of hard X-ray emission variations during flares in the energy range 25-35 keV if the relaxation time of electron density disturbances in the ionosphere of order 50-100 s is introduced. No such effect on the nightside of the Earth has been detected yet.

### 1 Introduction

The enhancement of X-ray and ultraviolet radiation intensity that is observed during chromospheric flares on the Sun immediately causes an increase in electron density in the ionosphere. These density variations are different for different altitudes and are collectively called Sudden Ionospheric Disturbances (SID). SID observations provide a key means for ground-based detection of solar flares along with optical observations of flares and solar radio burst observations. Much

research is devoted to SID studies, among them a number of thorough reviews and monographs [14].

Unlike effects in the optical and radio ranges, ionospheric effects of flares are of special interest as they constitute a response of ionospheric plasma to an impulsive ionization.

Quantitative study of SID has two major implications at present. SID data in the D-region that were obtained predominantly by recording amplitude and phase characteristics of signals from LF and VLF radio stations can be the source of information about the X-ray part of the flare spectrum, as well as providing a tool for investigating the principal chemical processes in this region.

SID data for the F-region acquired by different radio probing methods were used repeatedly to estimate time variations in the X-ray and extreme ultraviolet (EUV) spectral regions and in relative measurements of fluxes in different wavelength ranges [7]; [16]; [12]. The main body of SID data for the Earth's upper atmosphere was obtained in earlier detections of Sudden Frequency Deviations (SFD) of the F-region-reflected radio signal in the HF range [6]; [7].

SFD are caused by an almost time-coincident increase in E- and F-region electron densities at over 100 km altitudes covering an area with the size comparable to or exceeding that of the region monitored by the system of HF radio paths. A limitation of this method is the uncertainty in the spatial and altitude localization of the UV flux effect, the inadequate number of paths, and the need to use special-purpose equipment.

Another highly informative technique is the incoherent scatter (IS) method, one of the most universal tools for ionosphere research. In [16], important information was obtained about the height distribution of the decrease in local electron density  $N_e$  during the flares of May 21 and 23, 1967. A significant increase of  $N_e$  (by as much as 200 %) was recorded in the E-region, which decreased gradually in the F-region with an up to 10-30 % increase of the height and remained distinguishable up to 300 km.  $N_e$  starts to increase initially in the E-region, while at higher altitudes it is observed to be delayed, which is particularly conspicuous at the F-region heights.

The Millstone Hill IS facility recorded the flare of August 7, 1972 [13]. The measurements were made in the range from 125 to 1200 km, i.e. to the altitudes exceeding greatly those of all preceding observations. The increase of  $N_e$  amounted to 100 % at 125 km altitude and to 60 % at 200 km.

Implementing the IS method requires extremely sophisticated, expensive equipment. There are only a few IS facilities world-wide, which are concentrated mainly in America and Europe. These systems were designed for solving a broad gamut of scientific problems and do not provide round-the-clock observations of ionospheric effects from solar flares. An added difficulty involves inadequate time resolution. Currently it is common knowledge that the rise and fall time of the solar flare emission in the range 10-1030  $\mathring{A}$ , which has effect on the ionospheric - and F-regions, is often shorter than 5-10 min, typical of the IS method's time

resolution. Since the relaxation time of electron density in the E- and F1-regions is also less than 5-10 min, most incoherent scatter measurements lack adequate time resolution for studying ionospheric effects of flares.

The effect of solar flares on the ionospheric F-region is also manifested as a Sudden Increase of Total Electron Content (SITEC) which was measured previously using continuously operating VHF radio beacons on geostationary satellites [14]; [12].

In [12], a pioneering attempt was made to realize global observations of the outstanding flare of August 7, 1972 using 17 stations in North America, Europe, and Africa. The observations covered a territory whose boundaries were separated by 70° in latitude and by 10 hours in local time. For different stations, the value of dI (TEC increase) varied from  $1.8\,10^{16}$  <sup>-2</sup> to  $8.6\,10^{16}$  <sup>-2</sup>, or 15-30% of a total electron content. These investigations revealed a latitudinal dependence of the amount of TEC increase. The low latitudes showed a larger increase of TEC compared with the high latitudes. Besides, the authors point out no correlation between the value of TEC increase and the solar zenith angle.

A limitation of the SITEC method is the integral character of results which reflect the electron density variation in the height range from 100 to 2000 km. If, however, it is taken into consideration that only a few current methods enable flare effects to be recorded in the ionospheric F-region, SITEC observations should be recognized as one of the most convenient tools for continuous observations of the F-region.

A serious limitation of methods based on analyzing VHF signals from geostationary satellites is their small and ever increasing (with the time) number and the nonuniform distribution in longitude. Hence it is impossible to make measurements in some geophysically interesting regions of the globe, especially in high latitudes.

Consequently, none of the above-mentioned existing methods can serve as an effective basis for the radio detection system to provide a continuous, global SID monitoring with adequate space-time resolution. Furthermore, the creation of these facilities requires developing special-purpose equipment, including powerful radio transmitters contaminating the radio environment.

The advent and evolution of a Global Positioning System, GPS, and also the creation on its basis of widely branched networks of GPS stations (at least 600 sites at the end of 1999, the data from which are placed on the INTERNET) opened up a new era in remote ionospheric sensing. In the very near future this network will be extended by integrating with the Russian navigation system, GLONASS [11]. Furthermore, there exist also powerful regional networks such as the Geographical Survey Institute network in Japan [15] consisting of up to 1000 receivers. High-precision measurements of the group and phase delay along the line-of-sight (LOS) between the receiver on the ground and transmitters on the GPS system satellites covering the reception zone are made using two-frequency multichannel receivers of the GPS system at almost any point of the globe and

at any time simultaneously at two coherently coupled frequencies  $f_1 = 1575.42$  MHz and  $f_2 = 1227.60$  MHz.

The sensitivity of phase measurements in the GPS system is sufficient for detecting irregularities with an amplitude of up to  $10^{-3}$ – $10^{-4}$  of the diurnal TEC variation. This makes it possible to formulate the problem of detecting ionospheric disturbances from different sources of artificial and natural origins. Recently some authors embarked actively on the development of detection tools for the ionospheric response of powerful earthquakes [3], rocket launches [4], and industrial surface explosions [8]; [5]. Subsequetly, the GPS data began to be used in the context of the spaced-receiver method using three GPS stations to determine the parameters of the full wave vector of traveling ionospheric disturbances under quiet and disturbed geomagnetic conditions [1]; [2].

The objective of this paper is to develop a method of global detection of the ionospheric effect from solar flares (GLOBDET) using the international GPS network. This method would improve substantially the sensitivity and space-time resolution of analysis when compared with the above-mentioned radio probing methods. General information about the flares being analyzed here and a description of the experimental geometry are given in Section 2. The processing technique for the data from the GPS network and results of an analysis of the ionospheric effect from the solar flares of September 23, 1998 and July 29, 1999 are outlined in Section 3. Section 4 discusses the results obtained. A modeling of the physical processes involving flare effects on the ionosphere using GPS data and, moreover, the development of methods for solving their inverse problem of reconstructing emission characteristics using GPS data will be subject of future research.

## 2 Experimental geometry, and general data on the solar flares of September 23, 1998 and July 29, 1999

For studying the ionospheric response to the ionizing emission from solar flares, we chose relatively powerful (according to an X-ray classification) flares whose time profile was characterized by intense short-duration impulses of hard X-ray emission. The two flares selected appear in Table 1. The table also provides information about the characteristics of the CGRO- and YOHKOH-borne X-ray detectors, the data from which are compared with the ionospheric response to these flares in this paper.

Fig. 1 presents the geometry of a global GPS array used in this paper to analyze the effects of flare 23 September 1998 (102 stations – a.) and 29 July 1999 (105 station–b.). Heavy dots correspond to the location of the GPS stations. The coordinates of the stations are not given here for reasons of space. The upper

scales indicate the local time, LT, corresponding to 07:00 UT, a maximum increase in X-ray emission intensity of the flare 23 September 1998 and 19:30 UT for 29 July 1999 (see Section 3)).

As is evident from Fig.1, the set of stations which we chose out of the global GPS network available to us, covers rather densely North America and Europe, but provides much worse coverage of the Asian part of the territory used in the analysis. The number of GPS stations in the Pacific and Atlantic regions is even fewer. However, coverage of the territory with partial beams to the satellite for the limitation on elevations  $\theta > 10^{\circ}$ , which we have selected, is substantially wider. Dots in Fig. 1c mark the coordinates of subinospheric points for the height of the F2-layer maximum  $h_{max} = 300$  km for all visible satellites at 29 July 1999, 19:30 UT for each GPS station. A total number of beams (and subinospheric points) used in this paper to analyze the July 29, 1999 flare is 622.

Such coverage of the terrestrial surface makes it possible to solve the problem of detecting time-coincident events with spatial resolution (coherent accumulation) two orders of magnitude higher, as a minimum, than could be achieved in SFD detection on oblique HF paths. For simultaneous events in the western hemisphere, the correspoding today's number of stations and beams can be as many as 400 and 2000–3000, respectively.

Figs. 2b and 3b show the time dependencies of flare emission. Time profiles of soft X-ray emission were acquired by the GOES-10 satellite, the data from which are available on the SPIDER network (marked by the symbol o). Dashes in Figs. 2b and 3b represent values for the low-energy 1-8 $\mathring{A}$  channel. The time profile of the signal in the 0.5-4 $\mathring{A}$  channel was alike. A comparative analysis of these series is made in Section 6.

The study was based on events, for which flare emission data with a time resolution of about one second were available. The September 23, 1998 flare was recorded by X-ray telescope HXT on the YOHKOH satellite (Fig. 3b). Operating in the flare mode, the HXT telescope provides observations in four energy channels (14-23 keV, 23-33 keV, 33-53 keV, and 53-93 keV) with a resolution of 0.5 s. The second event was observed by the BATSE spectrometer on the CGRO satellite which is capable of recording solar X-ray emission with different temporal and spectral resolutions. This study utilized DISCLA data written in four channels (25-50 keV, 50-100 keV, 100-300 keV, and over 300 keV) at 1.024-second intervals.

The events are both characterized by a low level of geomagnetic disturbance (from -10 to -20 nT), which simplified greatly the SID detection problem.

# 3 Processing of the data from the GPS network, and results derived from analyzing the ionospheric effect from the solar flares of September 23, 1998 and July 29, 1999

Following is a brief outline of the global monitoring (detection) technique for solar flares (GLOBDET) as developed by one of the authors (Afraimovich E. L.) on the basis of processing the data from a worldwide network of two-frequency multichannel receivers of the GPS-GLONASS navigation systems.

A physical groundwork for the method is formed by the effect of fast change in electron density in the Earth's ionosphere at the time of a flare simultaneously on the entire sunlit surface. Essentially, the method implies using appropriate filtering and a coherent processing of TEC variations in the ionosphere simultaneously for the entire set of "visible" (during a given time interval) GPS satellites (as many as 5-10 satellites) at all global GPS network stations used in the analysis. In detecting solar flares, the ionospheric response is virtually simultaneous for all stations on the dayside of the globe within the time resolution range of the GPS receivers (from 30 s to 0.1 s). Therefore, a coherent processing of TEC variations implies in this case a simple addition of single TEC variations.

The detection sensitivity is determined by the ability to detect typical signals of the ionospheric response to a solar flare (leading edge duration, period, form, length) at the level of TEC background fluctuations. Ionospheric irregularities are characterized by a power spectrum, so that background fluctuations will always be distinguished in the frequency range of interest. However, background fluctuations are not correlated in the case of beams to the satellite spaced by an amount exceeding the typical irregularity size.

With a typical length of X-ray bursts and EUV emission of solar flares of about 5-10 min, the corresponding ionization irregularity size does normally not exceed 30-50 km; hence the condition of a statistical independence of TEC fluctuations at spaced beams is almost always satisfied. Therefore, coherent summation of responses to a flare on a set of beams spaced thoughout the dayside of the globe permits the solar flare effect to be detected even when the response amplitude on partial beams is markedly smaller than the noise level (background fluctuations). The proposed procedure of coherent accumulation is essentially equivalent to the operation of coincidence schemes which are extensively used in X-ray and gamma-ray telescopes.

If the SID response and background fluctuations, respectively, are considered to be the signal and noise, then as a consequence of a statistical independence of background fluctuations the signal/noise ratio when detecting the flare effect is increased through a coherent processing by at least a factor of  $\sqrt{N}$ , where N is the number of LOS.

It should be noted that because of the relatively low satellite orbit inclinations, the GPS network (and to a lesser degree GLONASS) provides poor coverage of the Earth's surface near the poles. However, TEC measurements in the polar regions are ineffective with respect to the detection of the ionospheric response to a solar flare because the amplitude of background fluctuations in this case is much higher when compared with the mid-latitude ionosphere. This is partiocularly true of geomagnetic disturbance periods. For the same reason, equatorial stations should also be excluded from a coherent processing.

The GPS technology provides the means of estimating TEC variations on the basis of phase measurements of TEC I in each of the spaced two-frequency GPS receivers using the formula [10]; [4]:

$$I = \frac{1}{40.308} \frac{f_1^2 f_2^2}{f_1^2 - f_2^2} [(L_1 \lambda_1 - L_2 \lambda_2) + const + nL]$$
 (1)

where  $L_1\lambda_1$  and  $L_2\lambda_2$  are phase path increments of the radio signal, caused by the phase delay in the ionosphere (m);  $L_1$ ,  $L_2$  is the number of full phase rotations, and  $\lambda_1$ , and  $\lambda_2$ , are the wavelengths (m) for the frequencies  $f_1$  and  $f_2$ , respectively; const is some unknown initial phase path (m); and nL is the error in determination of the phase path (m).

Phase measurements in the GPS system are made with a high degree of accuracy where the error in TEC determination for 30-second averaging intervals does not exceed  $10^{14}$   $^{-2}$ , although the initial value of TEC does remain unknown [10]. This permits ionization irregularitues and wave processes in the ionosphere to be detected over a wide range of amplitudes (as large as  $10^{-4}$  of the diurnal variation of TEC) and periods (from several days to 5 min). The TEC unit, TECU, which is equal to  $10^{16}$   $^{-2}$  and is commonly accepted in the literature, will be used throughout the text.

The solar flare of July 29, 1999 was used to illustrate the performance of the proposed method. Primary data include series of "oblique" values of TEC I(t), as well as the corresponding series of elevations  $\theta(t)$  and azimuths  $\alpha(t)$  along LOS to the satellite calculated using our developed CONVTEC program which converts the GPS system standard RINEX-files on the INTERNET [9]. The determination of SID characteristics involves selecting continuous series of I(t) measurements of at least a one-hour interval in length, which includes the time of the flare. Series of elevations  $\theta(t)$  and azimuths  $\alpha(t)$  of the beam to the satellite are used to determine the coordinates of subionospheric points. In the case under consideration, all results were obtained for elevations  $\theta(t)$  larger than  $10^{\circ}$ .

Fig. 4a presents typical time dependencies of an "oblique" TEC I(t) for the PRN03 satellite at the CME1 station on July 29, 1999 (thick line) and for PRN21 at the CEDA station (thin line). It is apparent from Fig. 4a that in the presence of slow TEC variations, the SID-induced short-lasting sudden increase in TEC is clearly distinguished in the form of a "step" as large as  $0.4\ TECU$ .

For the same series, similar lines in panel b. show variations of the time derivative of TEC dI(t)/dt with the linear trend removed and with a smoothing with the 5-min time window. The TEC time derivative is invoked because it reflects electron density variations which are proportional to the X-ray or EUV flux [14].

The dI(t)/dt variations for different beams are well correlated over the time interval from 19:30 to 19:39 UT. This is distinguished in a more instructive way if series of the time derivative dI(t)/dt for all visible satellites from 105 GPS stations are plotted on the same time scale (panel d). Time-coincident (for all beams) dI(t)/dt variations are clearly seen; for the remaining time spans of the time interval 19:00–20:00, UT variations of dI(t)/dt for different sites and satellites are not correlated and occupy the entire amplitude-time range.

The coherent summation of  $dI(t)/dt_i$  realizations was made by the formula

$$\sum dI(t)/dt = \sum_{i=1}^{N} dI(t)/dt_i sin(\theta_i)$$
(2)

where  $\theta_i$  is LOS elevation, i - number of LOS; i = 1, 2, ... N.

Multiplication by  $sin(\theta_i)$  was used to convert "oblique" TEC variations to an "equivalent" vertical value in order to normalize the response amplitude.

The normalized to N result of a coherent summation (2) for all beams and GPS stations located mainly on the dayside is presented in panel c. A comparison of the resulting coherent sum (2) with the time dependence dI(t)/dt for individual beams presented in panels b. and d. confirms the effect of a substantial increase of the signal/noise ratio caused by a coherent processing.

It is interesting to compare, for the same time interval, the data on individual beams and results from a coherent summation for the dayside and nightside. Fig. 4e presents typical time dependencies of an "oblique" TEC I(t) for the PRN27 satellite at the IRKT station (thick line) and for PRN27 at the BOGO station (thin line). Using the I(t) data it is impossible to identify any SID-induced short-lasting sudden increase in TEC. This is also true for the time derivatives dI(t)/dt plotted in panels f. and h. As a result, the r.m.s. of the coherent sum (2) in panel g. for the nightside is of the same order of magnitude as that of background fluctuations outside the SID response interval on the dayside, which is an order of magnitude (as a minimum) smaller than the SID response amplitude (Fig. 4c).

Consider the data processing procedure for the solar flare of September 23, 1998. Fig. 5 presents the time dependencies of TEC I(t) on the dayside – a. and dI(t) variations with the linear trend removed and smoothing with the 5-min time window for stations IRKT (PRN01) – b; dI(t) variations for all visible satellites from 102 GPS stations plotted on the same time scale – d. One can clearly see simultaneous (for all GPS beams) dI(t) variations; for the remaining

time spans of the interval 6:30-08:00 UT selected, dI(t) variations for different sites and satellites are not correlated and occupy the entire amplitude-time range.

It should be noted that in this case the ratio of the amplitude of the ionospheric response of the flare to the phase fluctuation amplitude is substantially worse than that for the flare of July 29, 1999. A preliminary coherent accumulation of  $dI(t)_i$ -series with a subsequent differentiation, rather than differentiation of single realizations of  $dI(t)_i$  with subsequent addition of the time derivatives seems more reasonable. The coherent summation of  $dI(t)_i$  realizations was made for this event by the formula

$$\Sigma dI(t) = \sum_{i=1}^{N} dI(t)_{i} sin(\theta_{i})$$
(3)

The (normalized to N) result of the coherent summation of series (3) for all beams and GPS stations located predominantly on the dayside is presented in panel c. Again, a comparison of the resulting coherent sum (3) with the time dependence of dI(t) for the individual beams shown in panels b. and d. confirms the enhancement effect of the signal/noise ratio beause of a coherent processing.

A similar result is also obtained by comparing (for the same time interval) the data from individual LOS and coherent summation results for the dayside and nightside. Fig. 5c presents typical time dependencies of an "oblique" TEC I(t) for the PRN14 satellite at station MAS1. The SID-induced short-lasting sydden increasze of TEC was not possible to identify from the I(t) data. This applies also for the dI(t)-variations with the trend removed, which are plotted in panels f. and h. As a result, the standard deviation (SD) of the coherent sum (3) in panel g. for the nightside is found to be of the same order o magnitude as the backgrund fluctuation SD outside the SID response range on the dayside, which is an order of magnitude, as a minimum, less than the SID response amplitude (Fig. 5c).

### 4 Discussion

A comparative analysis is made of the TEC data and X-ray emission time series acquired by satelites. In carrying out a comparative analysis of the TEC and X-ray emission to flares, it is necessary to eliminate the TEC trend which is not associated with flare emission. In this case the above procedure of determining the trend that is removed by a smoothing over a 5-min interval, which is significantly shorter than the flare emission duration, is incorrect. In Figs. 2 and 3, the trend to be removed was therefore defined as a polynomial of degree 3, approximating the time dependence of TEC on the intervals 19:00 and 20:00 UT, and 6:00-8:00 UT, respectively. The approximation procedure neglected the TEC values during the flares (19:30-19:48 UT, and 6:40-7:24 UT).

First we consider a simpler flare of July 29, 1999, with the X-ray emission time profile like a single impulse (dashed curve  $F_{HXT}$  in Fig. 2b). The flare is clearly seen on the time profile of TEC I(t) (Fig. 2a). As is apparent from Fig. 2b, the response  $I_{ex}(t)$  represents an impulse with a fast growth and a relatively slow decline. The time variation of soft X-ray emission, obtained from the GOES data at insufficiently large time intervals (marked by the symbol o in Fig. 2b) does not contradict the behavior of the curve  $I_{ex}(t)$ .

The rise front of hard X-ray emission  $F_{HXT}$  is steeper when compared with the response of TEC  $I_{ex}(t)$ , and the time of a maximum is 1.5 min ahead of the TEC fluctuation maximum. These difference are natural if account is taken of the finite relaxation time of electron density disturbances caused by flare emission. This factor can be taken into account by convoluting the source function  $F_{HXT}$  with the relaxation function:

$$F_{conv}(t) = \int_{0}^{t} F_{\mathsf{HXT}}(t') \exp\left[-\left(\frac{t - t'}{\tau}\right)\right] dt' \tag{4}$$

As is evident from Fig. 2c, the growth profile of TEC  $I_{ex}(t)$  is similar to that of the convolution  $F_{conv}$  when  $\tau = 65$  s. The convolution was accomplished with the X-ray signal of the 25-50 keV (0.25-0.5 A) energy channel. At the decay phase, the curves  $F_{conv}$  and  $I_{ex}(t)$  are moving apart, which can be associated with the contribution to the ionospheric ionization from softer emission whose time profile is similar to the GOES flux profile.

Short-duration disturbances on TEC dependencies, which are associated with the ionization by flare emission, are more pronounced on the time derivatives dI(t)/dt. Fig. 2d compares the result of summation (2) of the series of the derivatives  $\Sigma dI(t)/dt$  for all visible satellites from GPS stations located on the dayside, with the derivative  $d/dt(F_{conv})$  presented in Fig. 2c. It can be seen that the growth stage of the coherent sum  $\Sigma dI(t)/dt$  for the entire sunlit side of the Earth is described adequately by the function  $d/dt(F_{conv})$ . Note that the accuracy of estimating the duration  $\tau$  determined from the coincidence of peaks of the time derivatives is determined by time resolution of TEC measurements (30 s in the case under consideration).

The flare of September 23, 1998 was of a longer duration, and, despite a somewhat higher intensity, its response was relatively small on TEC time dependencies for separate paths (Fig. 3a). Nevertheless, by subtracting the polynomial of degree 3, it was possible to identify the TEC response  $I_{ex}(t)$  (Fig. 3b). In this event, the time dependence of soft X-ray emission is much different from the temporal behavior of the response  $I_{ex}(t)$  which grows faster than does the GOES signal (marked by the symbol o), attains a maximum 9 min earlier, and decreaes much more rapidly.

The signal of hard X-ray emission  $F_{HXT}$  (dashed line) shows a number of peaks leading the TEC fluctuations  $I_{ex}(t)$ . The convolution with the hard X-ray

emission signal  $F_{conv}$  agrees satisfactorily with the response  $I_{ex}(t)$ , with  $\tau = 100$  s. The curves in Fig. 2c are most similar for the M1 (22-35 keV) channel of the HXT/YOHKOH X-ray telescope. The estimated  $\tau = 100$  s is confirmed by comparing the combined time derivative of TEC  $\Sigma dI(t)/dt$ , with the derivative  $d/dt(F_{conv})$ .

A comparison of the time profiles of the TEC response and hard X-ray emission shows that corresponding electron density disturbances are recorded with confidence by a global GPS network. For hard X-ray emission, the highest correlation is attained for photon energies of about 30 keV, with relation times  $\tau$  in the range 65-100 s. These estimates are in reasonably good agreement with results obtained previously when analyzing the SID effect [7], [14].

Unfortunately, the lack of data on UV emission of the flares under investigation, the most probable ionizing factor at ionospheric heights above 100 km, gives no way of making absolute estimates of the TEC increment and comparing them with measured values. It is pointed out in [14] that although UV emission is essentially responsible for SID in the F-region, TEC variations are also correlated quite well with X-ray flares. This is also confirmed by simultaneous measurements of X-ray and EUV flare emission characteristics by the Solar Maximum Mission satellite [17].

### 5 Conclusions

In this paper we have analyzed the ionospheric response to powerful solar flares of September 23, 1998 and July 29, 1999. The analysis is based on implementing our new technology of a global detector of ionospheric effects from solar flares using the data from the international network of two-frequency multichannel receivers of the navigation GPS system (GLOBDET) which improves substantially the sensitivity and space-time resolution of observations over existing radio probing methods.

It was found that fluctuations of TEC and its time derivative obtained by removing the linear trend of TEC with a time window of about 5 min are coherent for all stations and beams to GPS satellites on the dayside of the Earth, regardless of the station's location, local time and elevation of the beam to the satellite. The time profile of TEC responses is similar to the time behavior of hard X-ray emission variations during flares in the energy range 25-35 keV if we introduce the relation time of an electron density disturbance in the ionosphere of a duration of 50-100 s. No such effect was detected on the nightside of the Earth.

The GLOBDET technology, suggested in this paper, can be used to detect small solar flares; the body of data processed is the only limitation in this case. The high sensitivity of GLOBDET permits us to propose the problem of detecting, in the flare X-ray and EUV ranges, emissions of nonsolar origins which are the result of supernova explosions.

For powerful solar flares like the one examined in this report, it is not necessary to invoke a coherent summation, and the SID response can be investigated for each beam. This opens the way to a detailed study of the SID dependence on a great variety of parameters (latitude, longitude, solar zenith angle, spectral characteristics of the emission flux, etc.). With current increasing solar activity, such studies become highly challenging. In addition to solving traditional problems of estimating parameters of ionization processes in the ionosphere and problems of reconstructing emission parameters [14], the data obtained through the use of GLOBDET can be used to estimate the spatial inhomogeneity of emission fluxes at scales of the Earth's radius.

### Acknowledgments

Authors are grateful to V. V.Grechnev, E. A. Kosogorov, O. S. Lesuta and K. S. Palamartchouk for preparing the input data. Thanks are also due V. G. Mikhalkovsky for his assistance in preparing the English version of the T<sub>E</sub>X-manuscript. This work was done with support from the Russian Foundation for Basic Research (grants 97-02-96060 and 99-05-64753), GNTP 'Astronomy' as well as RF Minvuz Grant 1999; supervisor B.O. Vugmeister.

### References

- [1] Afraimovich, E. L., K. S. Palamartchouk, and N. P. Perevalova, 1998. GPS radio interferometry of travelling ionospheric disturbances. Journal of Atmospheric and Solar-Terrestrial Physics 60, 1205–1223.
- [2] Afraimovich E. L., E. A. Kosogorov, L. A. Leonovich, K. S. Palamarchuk, N. P. Perevalova, and O. M. Pirog, Determining parameters of large-scale traveling ionospheric disturbances of auroral origin using GPS-arrays, Accepted by Journal of Atmospheric and Solar-Terrestrial Physics.
- [3] Calais E. and J. B. Minster, 1995. GPS detection of ionospheric perturbations following the January 1994, Northridge earthquake. Geophysical Research Letters 22, 1045–1048.
- [4] Calais E. and J. B.Minster, 1996. GPS detection of ionospheric perturbations following a Space Shuttle ascent, Geophysical Research Letters 23, 1897–1900.
- [5] Calais E., B. J. Minster, M. A. Hofton, and M. A. H. Hedlin, 1998. Ionospheric signature of surface mine blasts from Global Positioning System measurements. Geophysical Journal International 132, 191–202.

- [6] Davies K. *Ionospheric radio waves*, 1969. Blaisdell Publishing Company, A Division of Ginn and Company, Waltham, Massachusetts-Totonto-London.
- [7] Donnelly R. F, 1969. Contribution of X-ray and EUV bursts of solar flares to sudden frequency deviations. Journal Geophysical Research 74, 1873–1877.
- [8] Fitzgerald T. J., 1997. Observations of total electron content perturbations on GPS signals caused by a ground level explosion. Journal of Atmospheric and Solar-Terrestrial Physics 59, 829–834.
- [9] Gurtner, W., 1993. RINEX: The Receiver Independent Exchange Format Version 2. http://igscb.jpl.nasa.gov:80/igscb/data/format/rinex2.txt.
- [10] Hofmann-Wellenhof, B., H. Lichtenegger, and J. Collins, *Global Positioning System: Theory and Practice*, 1992. Springer-Verlag Wien, New York.
- [11] Klobuchar, J. A., 1997. Real-time ionospheric science: The new reality. Radio Science 32, 1943–1952.
- [12] Mendillo M., J. A. Klobuchar, R. B. Fritz, A. V. da Rosa, L. Kersley, K. C. Yeh, B. J. Flaherty, S. Rangaswamy, P. E. Schmid, J. V. Evans, J. P. Schodel, D. A. Matsoukas, J. R. Koster, A. R. Webster, P. Chin, 1974. Behavior of the Ionospheric F Region During the Great Solar Flare of August 7, 1972, Journal Geophysical Research 79, 665–672.
- [13] Mendillo M., and J. V. Evans, 1974. Incoherent scatter observations of the ionospheric response to a large solar flare. Radio Science 9, 197–203.
- [14] Mitra A. P., 1974. Ionospheric effects of solar flares, New Delhi -12, India.
- [15] Saito A., S. Fukao and S. Miyazaki, 1998. High resolution mapping of TEC perturbations with the GSI GPS network over Japan. Geophysical Research Letters 25, 3079–3082.
- [16] Thome G. D and L. S. Wagner, 1971. Electron density enhancements in the E and F regions of the ionosphere during solar flares. Journal Geophysical Research 76, 6883–6895.
- [17] Vanderveen K., L. E. Orwig, and E. Tandberg-Hanssen, 1988. Temporal correlations between impulsive ultraviolet and hard X-ray busts in solar flares observed with high time resolution, Astrophysical Journal 330, 480–492.

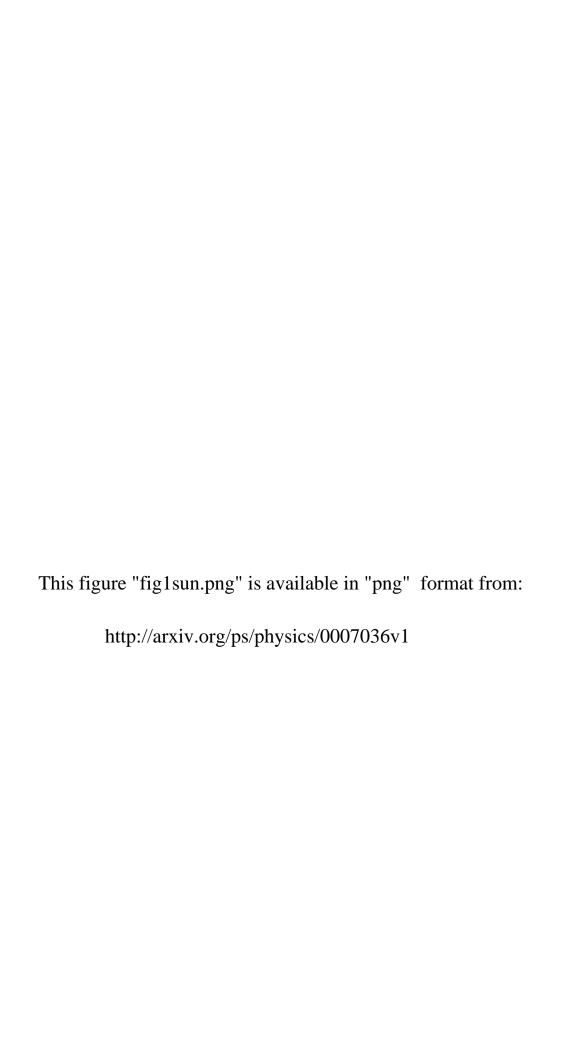


Table 1: Parameters of the flares being analyzed

N		September 23, 1998	July 29, 1999
1	Time of maximum		
	soft X-ray emission, UT	07:13	19:34
2	Flare class		
	optical/X-ray	3B/M7.1	1N /M5.1
3	X-ray class with the highest	НХТ/ҮОНКОН)	$\mid$ CGRO/BATSE $\mid$
	degree of correlation	M1(22-35  keV)	$25\text{-}50~\mathrm{keV}$
4	Increment of electron		
	content, TECU	0.4	0.5
5	Relaxation time, s	100	65

